

Domain Coarsening in Systems Far from Equilibrium

M. C. Cross and D. I. Meiron

Condensed Matter Physics and Applied Mathematics, Caltech, Pasadena, California 91125

(Received 27 April 1995)

The growth of domains of stripes evolving from random initial conditions is studied in numerical simulations of models of systems far from equilibrium such as Rayleigh-Bénard convection. The size of the domains deduced from the inverse width of the Fourier spectrum is found to scale as $t^{1/5}$ for both potential and nonpotential models. The morphology of the domains and the defect structures are, however, quite different in the two cases, and evidence is presented for a second length scale in the nonpotential case growing as $t^{1/2}$.

PACS numbers: 64.60.Cn, 47.20.Bp

When a system is quenched through a transition from a disordered to an ordered state small domains of the different symmetry manifestations of the ordered phase initially form. These then grow to give larger ordered regions, asymptotically approaching the ideal of very large ordered regions. There has been a great deal of study of this *coarsening* process in systems where the different states are equilibrium thermodynamic phases at finite temperature. In this paper we extend this question to systems in which the “ordered” state is produced by a pattern forming instability in a system far from equilibrium (the canonical example being Rayleigh-Bénard convection).

We investigate the formation of a “stripe” state in two dimensions, with rotational invariance in the plane. Rayleigh-Bénard convection is such a system, with the stripes corresponding to the familiar convection rolls. After a quench into the ordered region, given by stepping the Rayleigh number (the dimensionless temperature difference across the depth of the cell driving the convection), regions of differently oriented stripes grow from random initial fluctuations as the dynamics rapidly drives the system locally to a state with the characteristic length scale of the stripes. The questions that arise are how does the length scale over which the stripes are ordered grow, and what are the scaling properties, for example, characterized by the structure factor. In addition, because of the stripe nature of the ordered state, there is the question of what is the large scale morphology; for example, is it best described as domains of rather straight stripes with sharp domain boundaries between them (i.e., a pattern of grains), or are the stripes curved on the large length scale. (This same question would arise in the quenching into an equilibrium stripe phase such as a two-dimensional smectic.) For the system far from equilibrium there is also the question of “wave-vector selection,” i.e., what is the long time asymptotic wavelength of the stripe pattern. Note that for a thermodynamic equilibrium phase the asymptotic wave vector will simply be the one that minimizes the free energy. For a stripe state far from equilibrium there is no corresponding argument, and indeed the question of wave-vector selection has aroused considerable interest.

In this paper we study the formation of the stripe phase in numerical simulations of equations that model Rayleigh-Bénard convection. These equations are based on the Swift-Hohenberg equation that was introduced [1] to look at the effect of fluctuations on the transition to the convective roll state. It is an equation for a real order parameter $\psi(\vec{r}, t)$ that is a function of the horizontal coordinates $\vec{r} = (x, y)$ and time t . In a uniform convective state of straight parallel rolls ψ takes the form

$$\psi \propto \cos(\vec{q} \cdot \vec{r} + \phi) + \text{harmonics}, \quad (1)$$

with \vec{q} the wave vector of the stripes and ϕ the phase variable, and gives the horizontal variation of the pattern that is involved in questions of pattern formation. Swift and Hohenberg were interested in universal aspects of the transition, and so wrote down the simplest dynamical equation consistent with the symmetries and the existence of a stripe state,

$$\dot{\psi} = \epsilon\psi - (\nabla^2 + 1)^2\psi - \psi^3 + \eta(\vec{r}, t), \quad (2)$$

with the dot denoting a time derivative and ∇^2 the two-dimensional Laplacian. Here ϵ is the control parameter, depending linearly on the temperature difference driving the convection, with the transition to stripes occurring for $\epsilon > 0$, and η is a noise term that was introduced to investigate the effect of thermal fluctuations on the transition. Equation (2) also describes a near equilibrium system, since the dynamics are “potential,” i.e., follow the descent of a potential functional, which would be the free energy for the near equilibrium system. Equation (2) has since been much used as a useful qualitative model of features of pattern forming systems that may not be quantitatively universal, since it incorporates the three important features of such systems, namely, growth of the disturbance, nonlinear saturation, and dispersion. However, the potential aspect of the dynamics is not appropriate for systems far from equilibrium, and so various modifications have been proposed to account for this aspect. In particular, Greenside and Cross [2] suggested a modification of the nonlinear term to yield

$$\dot{\psi} = \epsilon\psi - (\nabla^2 + 1)^2\psi + 3(\vec{\nabla}\psi)^2\nabla^2\psi. \quad (3)$$

As well as being nonpotential, this equation also gives a better representation of the stability of the stripe phase as the wave vector and control parameter are varied (the “stability balloon”) for convection [2]. A further model is given by incorporating the effects of mean drift. In the convection system a mean flow (averaged over the depth of the cell), slowly varying with the horizontal coordinates, is an important additional degree of freedom that qualitatively changes the physics [3,4]. This leads to the equations

$$\begin{aligned} \dot{\psi} + \vec{U} \cdot \vec{\nabla} \psi &= \epsilon \psi - (\nabla^2 + 1)^2 \psi + \text{NL}, \\ \vec{\nabla} \times \vec{U} &= \Omega \hat{z}, \end{aligned} \quad (4)$$

$$\tau_v \dot{\Omega} - \sigma (\nabla^2 - c^2) \Omega = g_m \hat{z} \cdot \vec{\nabla} (\nabla^2 \psi) \times \vec{\nabla} \psi,$$

where $\vec{U}(x, y, t)$ is the divergence-free horizontal velocity that advects the field ψ in the first equation (with the symbol NL referring to either of the nonlinearity choices). The velocity \vec{U} is defined in terms of the vertical vorticity Ω , which is in turn driven by distortions of the stripe pattern through the third equation. Here g_m gives the coupling between the mean flow and the stripes, and increases as the Prandtl number (the ratio of viscous to thermal diffusivities) decreases. The parameters τ_v , σ , and c may be chosen to match the fluid system: we use $\tau_v = 1$, $\sigma = 1$, and $c^2 = 2$. We will present results for $\epsilon = 0.5$ for Eqs. (3) and (4), and $\epsilon = 0.25$ in Eq. (2) since the dynamics appears to freeze at long times in this model for the higher value.

Coarsening in the Swift-Hohenberg equation has been studied by Elder, Vinals, and Grant [5]. In the presence of the noise term (corresponding to a finite temperature thermodynamic system) their numerics yielded a length scale increasing with time as $t^{1/4}$. In the absence of noise they found a slower growth, consistent with a $t^{1/5}$ scaling. These results are surprising at first sight, since the long time dynamics of the system is governed by the “phase diffusion equation,” an equation for the slow space and time variation of the phase ϕ introduced in Eq. (1),

$$\dot{\phi} = D_{\parallel} \partial_{\parallel}^2 \phi + D_{\perp} \partial_{\perp}^2 \phi, \quad (5)$$

where \parallel and \perp refer to directions parallel and perpendicular to the local wave vector, and $D_{\parallel}(q)$ and $D_{\perp}(q)$ are diffusion constants that depend on the local wave number $q = |\vec{\nabla} \phi|$. Simple power counting leads to a length scale growing asymptotically as $\xi \sim t^{1/2}$. Earlier, however, Cross and Newell [6] had proposed that on long time scales the local wave number should tune itself to a value q_f for which $D_{\perp} = 0$, so that the second term in Eq. (5) drops out. In addition, the first term in Eq. (5) is also zero since $\partial_{\parallel} \phi = q$ is then constant. Cross and Newell proposed that higher order gradient terms in the phase equation would control the dynamics. In the original paper they suggested a scaling $\xi \sim t^{1/3}$, but more recently Cross and Hohenberg [7] suggested $t^{1/4}$ as the correct result of this analysis, closer to the results of the numerics [8]. The tuning of the wave number to q_f follows directly for potential systems, since this wave number is also the one that minimizes the

potential. However, Cross and Newell suggested that this was also valid more generally, since, in the absence of coupling to mean drift, focus singularities also relax the wave number to this value. (A focus singularity is the center of curvature of axisymmetric stripes or a sector of such stripes, and permits the disappearance or nucleation of stripes driven by curvature effects until $D_{\perp} \rightarrow 0$.) This tuning does not survive the coupling to mean flow effects. Thus at the outset of this work we expected to find a $t^{1/4}$ or $t^{1/5}$ scaling for the nonpotential case Eq. (3) with a concomitant approach of the mean wave number to q_f , but a different scaling, perhaps $t^{1/2}$, with the addition of mean flow.

We now summarize our results. We find a slow evolution of the characteristic length scale ξ_q , defined from the width of the wave-vector distribution in Fourier space, consistent with $\xi_q \sim t^{1/5}$ for *all three* cases studied: potential, nonpotential, and with the inclusion of mean flow (also nonpotential). For the nonpotential cases, a second length scale ξ_r defined from the correlations of the orientation of the stripes in real space (a less accurate calculation) appears to show a different scaling consistent with $\xi_r \sim t^{1/2}$. In the nonpotential cases the asymptotic wave number does *not* approach the value q_f at which D_{\perp} is zero. Rather it seems to approach closely the wave number at which isolated dislocations are stationary. The morphology of the pattern appears quite different in the potential and nonpotential cases (see Fig. 1). For the potential equation the pattern [panel (a)] may be described as

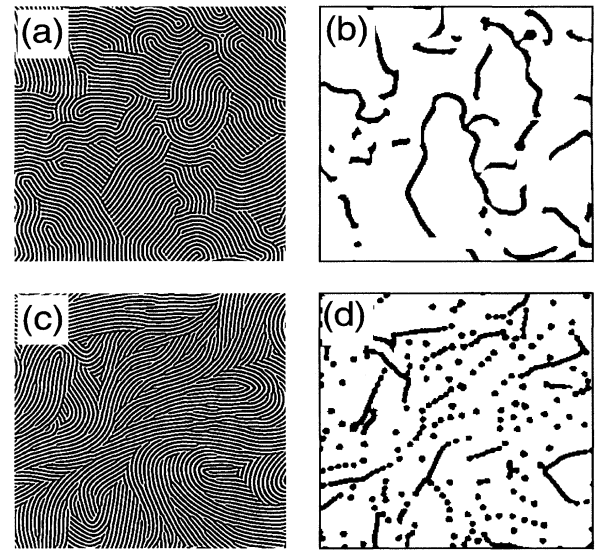


FIG. 1. Morphology of the stripe pattern in (a) potential and (c) nonpotential models of convection during the coarsening process, with black and white denoting positive and negative values of the field ψ . The pictures show one quarter of the actual system used. Panels (b) and (d) show the corresponding defect structure visualized as the regions where the amplitude of the stripe pattern (calculated using Fourier filtering methods) falls below 75% of the maximum value.

largely consisting of domains of straight stripes with sharp boundaries between the domains, although there are also some regions where a smoother variation of the stripes is seen. Two kinds of domain walls may be identified: lines where one set of stripes ends and a second set starts, visible in panel (b); or lines where there is a sharp kink in the stripe orientation, but a smaller perturbation of the amplitude so that there is no signature in panel (b). For the nonpotential equation stripes smoothly curved over the characteristic scale are evident [panel (c)], and isolated dislocation defects are more apparent [see also panel (d)].

The variation of the length scale ξ_q with time is shown in Fig. 2, showing results from our longest runs (times to 7400) and largest systems (around 1000 in size). These results were produced from random initial conditions (independent random numbers on each mesh point) with a time step of 0.2, after an initial transient of time length 1 integrated with time step 0.01 to allow the large wave-vector components of the initial condition to decay. The numerical scheme was a pseudospectral scheme using 1024×1024 Fourier modes with second order accurate time stepping described previously [9], with periodic boundary conditions. Each integration step took 0.5–1 sec (depending on the complexity of the nonlinear term in the equation) on one processor of a Cray C90.

Figure 2 shows the time variation of the “width” δq of the structure factor $S(q, t) = \langle \psi(\vec{q}, t) \psi(-\vec{q}, t) \rangle$ in Fourier space, with both axes on logarithmic scales. The average $\langle \rangle$ is over angles of the wave vector \vec{q} , and the data represent a single run, although other runs were done with consistent results. We extract the width δq from a Lorentzian squared fit

$$S(q) = \left(\frac{a}{(q^2 - b)^2 + c^2} \right)^2, \quad (6)$$

with δq defined as the half width at half height $\delta q = 0.322c/\sqrt{b}$. Although this fit does show systematic

deviations, it yields values of δq that are insensitive to the range of the fit. (We have used a range $\pm 4\delta q$.) For both the potential Swift-Hohenberg model (as seen earlier by Elder, Vinals, and Grant [5]) and the nonpotential model, the long time variation is well fit by a power law $\delta q \propto t^{-1/5}$ over two or more decades in time [10]. This same scaling was found including the mean flow: We used vorticity coupling constants $g_m = 10$ and $g_m = 20$ with $\tau_v = 1$, $c^2 = 2$, $\sigma = 1$, in a smaller system size of about 536 with a 512×512 mesh because of the increased numerical complexity, and to shorter times (about 4000) to eliminate finite size saturation effects. The results remain consistent with a power law scaling of around $\frac{1}{5}$, and are clearly not consistent with a $t^{1/2}$ scaling.

We can also wonder whether the patterns are characterized by a single (long) length scale. To investigate this question we have calculated the stripe orientation field correlation function. The Fourier space filtering method to extract the local orientation $\theta(\vec{r}, t)$ of the stripes has been described previously [9]. We then calculate $C_2(|\vec{r} - \vec{r}'|, t) = \langle e^{i2[\theta(\vec{r}, t) - \theta(\vec{r}', t)]} \rangle$, averaging over the spatial coordinates \vec{r} and \vec{r}' for fixed $r = |\vec{r} - \vec{r}'|$ for each time t . As expected the correlations decay with increasing separation r , and from this decay we can extract a characteristic length $\xi(t)$. (We have chosen to use simply the half width at half height of C_2 , since the quality of the data and the limited range of r probed due to the finite size of the system do not warrant a functional fit to the decay.) Interestingly, for the potential Swift-Hohenberg model we find that the variation of ξ is roughly consistent with δq^{-1} from the width of the structure factor (the fit shown in the inset to Fig. 2 over a relatively small range of times gives $\xi \sim t^{0.24}$). On the other hand, for the nonpotential model the variation is close to $\xi \sim t^{1/2}$ rather than the $t^{1/5}$ for δq^{-1} . Inspecting the domain morphology from Fig. 1, or better from a plot of the orientation field $\theta(\vec{r})$, suggests that in the nonpotential case there may be stronger correlations along the stripes than perpendicular to the stripes. We might expect the latter to have a stronger influence on the range of wave numbers in the pattern that determines δq .

An important question that has aroused much interest in nonequilibrium stripe states is the question of wave-vector selection, i.e., is there a preferred wave vector for each set of control parameters that is selected in patterns under a wide range of situations such as different geometries or initial conditions. One popular hypothesis in the literature has been the “maximum growth rate” idea, namely, that the wave vector selected is the one that has the maximum growth rate in the linear (small amplitude) regime. More recently the importance of the nonlinearity of the system has been studied, mainly in two classes of situations: the evolution from random initial conditions in a *one-dimensional* geometry; and geometrically simple situations in one or two dimensions, for example, concentric stripes, or patterns with one or two defect structures such as dislocations or grain boundaries (see Ref. [7] for a review). The present

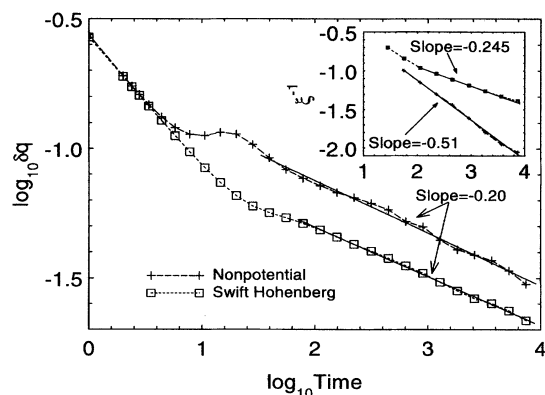


FIG. 2. Plot of the logarithm of the inverse length scale as a function of log time for the potential (squares) and nonpotential (crosses) models. The main figure shows the width of the structure factor; the inset shows the inverse of the half width of the decay of the orientation field correlation function in real space.

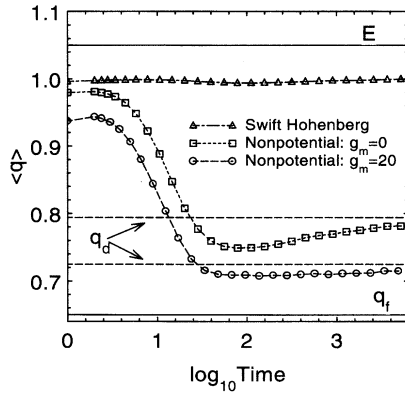


FIG. 3. Evolution of the mean wave number with logarithmic time for the potential Swift-Hohenberg model (triangles), the nonpotential model (squares), and the nonpotential model with added mean flow (circles). Also shown are some characteristic wave numbers for the nonpotential model: E —the wave number at which the stripes become unstable to the longitudinal (Eckhaus) instability; q_f —the wave number selected by focus defects at which D_{\perp} goes to zero in the absence of mean flow; and q_d —the wave number at which the climb velocity goes to zero, shown for the two values of the vorticity coupling used in the plot.

situation combines aspects of both of these: we start from random initial conditions, but also the evolution leads to states with defects that allow wave-number relaxation. In the potential case all results have shown that the wave vector that minimizes the potential is selected in all cases. For the Swift-Hohenberg model at $\epsilon = 0.25$ this is very close to $q = 1$, and indeed we see, Fig. 3, that the mean wave number is very close to this value over the whole time period. For the nonpotential cases the evolution is much more interesting. Although a value $q \approx 1$ is produced by the early evolution where the biharmonic operator tends to filter out other wave numbers in the linear evolution (i.e., consistent with the maximum growth rate idea), at later times there is a trend to smaller wave vectors, and then a slow increase to a long time asymptotic value away from unity. Empirically we find that the wave number at long times approaches a value that is very close to the wave number q_d at which isolated dislocation defects are stationary, i.e., have zero climb velocity. (These values are obtained by separate runs measuring the climb velocity of a defect pair in otherwise straight stripes at various wave numbers, and the wave number for zero climb velocity is found by interpolation.) The relevance of the dislocation selected wave number is confirmed by the agreement of the asymptotic wave

number with q_d for the two different values of g_m , as shown in Fig. 3.

We do not have a good theoretical understanding of these results. In the potential case, a dimensional analysis of the phase equation might be argued to lead to a $t^{1/4}$ scaling since the diffusion constant tends to zero as the wave number approaches its long time asymptote. Although this result was found by Elder, Vinals, and Grant [5] in the case with added noise, both they and we find a slower dependence in the absence of noise, although the expectation [11,13] is that noise should be irrelevant to the long time, large scale dynamics. Recent work [12] has suggested the importance of defects in the coarsening process leading to corrections to this naive result. The defect structure of stripe phases is complicated, and understanding the role of the various defects in the coarsening process as well as an extension of these ideas to the nonpotential case remain challenges for the future. We also hope experiments on larger aspect ratio systems than to date may test these ideas.

This work was supported by the National Science Foundation through Grant No. DMR-9013984, by the DOE through Grant No. DE-FG03-89ER25073, and by a generous award of computer time from the San Diego Supercomputer Center. We thank David Huse for useful discussions.

-
- [1] J.B. Swift and P.C. Hohenberg, Phys. Rev. A **15**, 319 (1977).
 - [2] H.S. Greenside and M.C. Cross, Phys. Rev. A **31**, 2492 (1985).
 - [3] E.D. Siggia and A. Zippelius, Phys. Rev. A **24**, 1036 (1981).
 - [4] M.C. Cross, Phys. Rev. A **29**, 391 (1984).
 - [5] K.R. Elder, J. Vinals, and M. Grant, Phys. Rev. Lett. **68**, 3024 (1992).
 - [6] M.C. Cross and A.C. Newell, Physica (Amsterdam) **10D**, 299 (1984).
 - [7] M.C. Cross and P.C. Hohenberg, Rev. Mod. Phys. **65**, 851 (1994).
 - [8] Elder, Vinals, and Grant [5] also suggested a $t^{1/4}$ scaling for an intermediate time range.
 - [9] M.C. Cross, D. Meiron, and Y. Tu, Chaos **4**, 607 (1994).
 - [10] Other functions, such as $t^{-1/4}/\log t$ give equally good fits.
 - [11] A.J. Bray, Phys. Rev. Lett. **62**, 2841 (1989).
 - [12] C.W. Meyer, G. Ahlers, and D.S. Cannell, Phys. Rev. A **44**, 2514 (1991).
 - [13] A.J. Bray and A.D. Rutenberg, Phys. Rev. E **49**, R27 (1994); A.D. Rutenberg and A.J. Bray (unpublished).